

Fig. 1: Histogram of asteroid rotation periods as published until 1982; numbers and names for slowly spinning asteroids with periods longer than 50 hours are given. The long rotation period $P = 145.0$ hours for 1689 Floris-Jan is clearly exceptional.

rates. In addition, it must be stated that – in opposition to what should be expected – there are indications that small asteroids are not necessarily fast rotators. Among all asteroids with rotation periods longer than 50 hours there appear to be no objects larger than 100 km. It is still premature for a final conclusion, but it seems that small asteroids prefer also slow rotation rates, whereas larger objects with diameters larger than 200 km (roughly 30

asteroids) prefer to rotate faster with periods of the order of only 8–29 hours!

We are waiting even for other surprises: 1981 QA, also a small asteroid with a 0.8–2 km size is reported to rotate also in only six days approximately – and new exciting results are to be expected for 288 Glauke, a 30 km sized S-type asteroid.

Good luck for all hunters!

The Atmospheric Transmission at La Silla at 230 GHz

J. Brand, Sterrewacht Leiden

Introduction

From April to November 1981, ESO La Silla was host to a team of observers from the Netherlands, forming the "CO group". During this time they applied themselves to detecting radiation of the CO molecule at 230 GHz, using the CAT and their own heterodyne (sub-)millimetre wave receiver.

In general the importance of CO observations lies in the fact that CO is, after molecular hydrogen, the most abundant molecule in interstellar space while its (dipole) rotational transitions can be much more easily detected than the very weak (quadrupole) rotational transitions of H_2 ; the rotational levels of CO are believed to be excited by collisions with other particles, mostly H_2 , and therefore, by studying the distribution and kinematics of CO one gets indirect information on those properties of H_2 .

So far, most information on the distribution of molecular clouds in the Galaxy is based on observations of the ^{12}CO $J = 1 \rightarrow 0$ rotational transition at 115 GHz. Such observations have been carried out mainly from northern hemisphere observatories and were therefore limited to $\delta > -40^\circ$. Incidental observations from the southern hemisphere have been made using optical telescopes, due to

the lack of mm telescopes. As the CAT, being just installed, was not yet scheduled for general use, ESO agreed to allocate us all day time and about half of the night time in the above-mentioned period. We have used this telescope to survey the galactic plane in the fourth quadrant, to observe molecular clouds associated with HII regions and to make maps of a few dark clouds. Since this was the first time the CAT was used so extensively, we encountered several telescope problems. Pointing, for instance, was off by a few degrees in some directions. Extensive star pointing sessions showed the offset to be systematic and a correction programme was developed bringing the absolute pointing accuracy 1 to 2. This problem is less serious for observers using the spectrograph since the stars can be seen on the TV screen and thus centered (the correction programme is also implemented for these observers, however); the tracking capability of the CAT is good.

Other problems arose from the fact that the CAT was not designed for this type of operation. The most persistent of these typically frequency-related problems is the reflection of local oscillator signal from the receiver on dome and telescope surfaces, causing variable standing waves in the spectra. We were able to suppress these

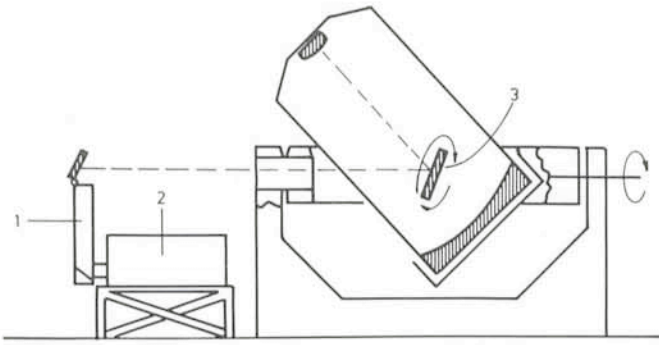


Fig. 1: The ESTEC sub-mm heterodyne receiver as it was installed in the CAT dome. The light coming from the Nasmyth mirror in the telescope is reflected into the receiver by the flat mirror on top of the aluminium tube. Cables carrying the signal from the receiver to the computer (not shown) are guided through the light tunnel connecting the CAT building with that of the 3.6 meter telescope (drawing of telescope adopted from ESO Users Manual). 1. Aluminium tube, with polyethylene lens (not visible) and flat mirror. 2. ESTEC receiver. 3. Nasmyth mirror.

standing waves to some extent by putting mm-wave-absorbing material around the secondary mirror turret and using a wobbling mirror inside the receiver.

At our observing frequency of 230 GHz atmospheric water vapour is the main absorbant. The dry climate at La Silla allows this radiation to pass through the atmosphere without too much attenuation. In this paper we give information on the atmospheric condition during our stay at La Silla, monitored by means of skydipping procedures.

General System Description

The receiver has been built at ESTEC (Nordwijk, the Netherlands) in collaboration with the observatory at Utrecht and it has been in operation since 1978. It can be tuned within the frequency range 200 to 400 GHz, which

corresponds to wavelengths between 1.5 and 0.75 mm. In this range many of the essential rotational transitions of the light molecular species are situated. In the receiver the signal is brought down to a lower, intermediate frequency (about 1.2 GHz), for which suitable (i.e. low noise and high resolution) detection devices exist. Down conversion is accomplished by mixing the incoming signal with a local oscillator signal at about the same frequency; mixing takes place in a non-linear element, in our case a room temperature Schottky barrier diode. Details of the receiver and its operation are given by Lidholm and de Graauw (1979).

For detection, the signal is fed into two 256-channel filterbanks, with a width per channel of 1 MHz and 250 kHz respectively, corresponding to 1.3 kms⁻¹ and 0.3 kms⁻¹ velocity resolution. The available velocity ranges are respectively 333 kms⁻¹ and 83 kms⁻¹ (both centered at the same velocity). A computer integrates the signals from the filterbanks and the result is stored on magnetic disk. Our data-taking computer also contains a telescope pointing programme and mapping routines and was linked to the CAT computer allowing us to operate the telescope from our control room and to carry out long observing sessions without having to interfere. Observations were made in the position switching mode, where the signal from a reference position is subtracted from that of the source position, resulting in the net signal from the source position, relative to a zero baseline level. Typically, one pair of source-reference measurements takes 2 × 100 sec.

Fig. 1 shows the CAT/ESTEC receiver combination during operation.

Atmospheric Transmission

Atmospheric transmission can be derived from a so-called "skydip", in which the telescope is pointed at several successive elevations, all at the same azimuth. In our case a skydip usually consisted of measurements at

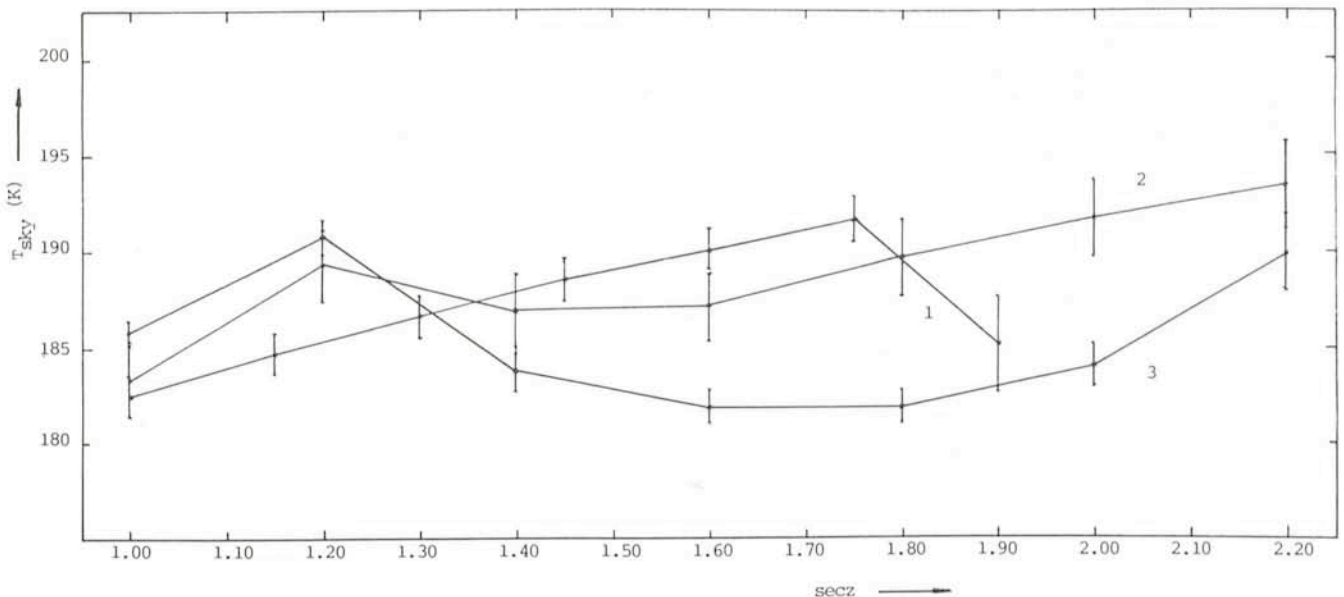


Fig. 2: Three characteristic skydip results (sky temperature vs. secz): series 1: Az = 210° (SW); series 2 and 3: Az = 90° (E) (series 3 shows a partly inverted atmospheric temperature profile).

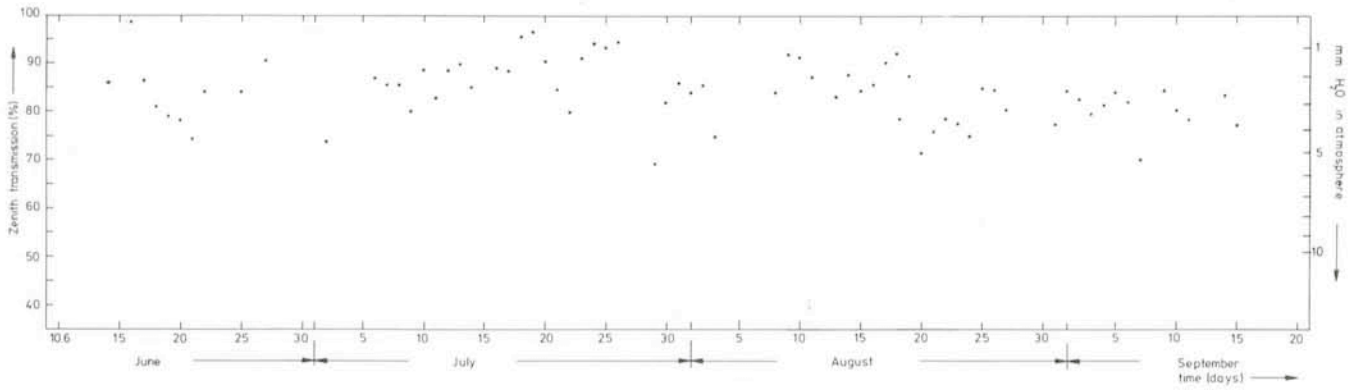


Fig. 3: Average daily zenith transmission (left-hand scale) and atmospheric water vapour content (right-hand scale) derived under the assumption of a constant efficiency of 35% as a function of time. Gaps indicate days we did not observe. This was mostly due to windspeeds of more than 100 km h^{-1} . Other causes were: check-up of equipment and re-alignment (30/6 and 1/7); humidity close to 100% (3/8 to 7/8, and 30/8); snow and ice (12/9 and 13/9).

six elevations, covering the interval $\text{secz} = 1$ (elevation = 90° ; $z = \text{zenith distance}$) to $\text{secz} = 2$ (elevation = 30°). Higher values of secz (lower elevations) cannot be reached because of the construction of the CAT.

At each elevation the signal from the sky is compared with the signal from a piece of "eccosorb" absorber at ambient temperature ($\sim 285 \text{ K}$), giving the sky brightness temperature. From those observations, the optical depth of the atmosphere at zenith and an efficiency factor (accounting for losses in the telescope and for radiation entering the receiver from directions other than that of the source) can be determined, by fitting a theoretical curve through the data with these two unknowns as free parameters. This procedure assumes an exponential relation to exist between sky brightness temperature and secz . During our stay at La Silla we made over 200 skydips, providing information on atmospheric conditions in the period 14 June to 15 September 1981 (the October and November data have not yet been reduced). In Fig. 2 we show characteristic skydip results for two different azimuths. The measured points are indicated by filled circles. For reasons of clarity points pertaining to the same dip have been connected by straight line sections. (Each point is an average over several measurements; the vertical bars indicate the uncertainty in this average.)

Series 1 is the average of a number of skydips performed at azimuth = 210° (direction SW; azimuth (Az) is defined here as being 0° to the north and increasing from N to E).

Series 2 and 3 show characteristic dips at Az = 90° (east). Seventy-two per cent of all skydips were performed in the SW direction, and nearly all of these (96%) feature a smooth increase of sky temperature with increasing secz , as illustrated by series 1. In all these cases a satisfactory fit to the data could be made. The efficiency factor was found to be $0.35 (\pm 0.03 \text{ s.d.})$. All remaining skydips (28% of the total) were performed to the east. The majority of these (62%) show a run of sky temperatures with secz as series 3, which is partly inverted. Since in this case the assumed exponential relation between temperature and secz is absent, no meaningful values for zenith opacity and efficiency factor can be derived from these by our fitting procedure. Therefore it was assumed that the same efficiency factor applies to skydips performed at different azimuths, leaving only one unknown (the zenith opacity) in the fitting procedure. All formerly unsolvable eastern skydips have been reduced along this

line. The zenith opacities thus obtained were transformed into atmospheric transmission percentages and shown in Fig. 3. Also indicated is the corresponding amount of H_2O in the atmosphere (using $\tau = 0.067/\text{mm H}_2\text{O}$; van de Stadt, internal memo). The data in Fig. 3 are average daily (0:00 UT – 24:00 UT) transmissions. The absolute uncertainty in these numbers is about $\pm 5\%$. We have not observed every day during the indicated period; gaps in Fig. 3 indicate days during which we could not observe at all. This was usually due to windspeeds of more than 100 km h^{-1} under which circumstances we were not allowed to open the dome. Other causes that play a role are time lost through check-up of our equipment and re-alignment, humidity close to 100% and precipitation (snow and ice). Apart from weather conditions on a particular day, the number of points that make up a "daily average" in Fig. 3 also depends on whether observing time was allocated to us 24 hours a day or only during daytime. In short, Fig. 3 gives a representative picture since we did not observe only when ESO regulations did not allow us to; the data are not biased by picking out days with seemingly good

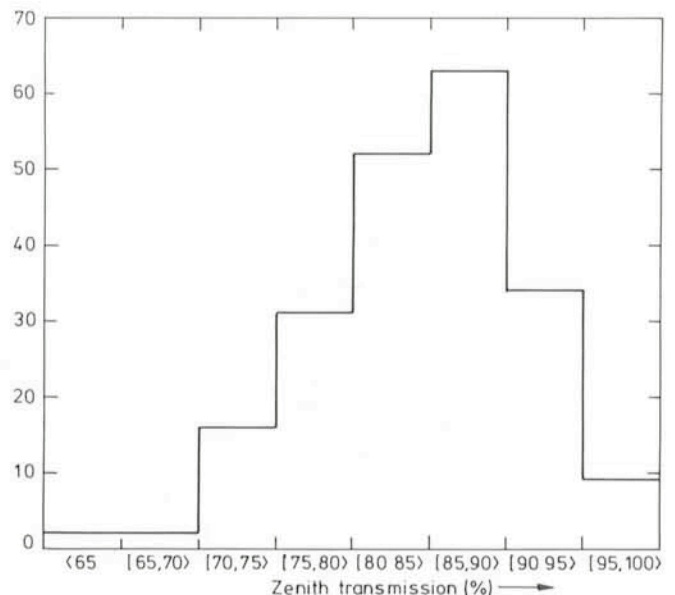


Fig. 4: Distribution of zenith transmissions from individual skydips (assuming a constant efficiency of 35%).

observing conditions only. It can be seen that in general over the indicated period of time atmospheric transmission at 230 GHz was quite good, roughly between 80 % and 90 %, as can be seen more clearly from Fig. 4, which shows the distribution of zenith transmissions. The lowest transmission obtained from individual skydips are 46 % and 57 %. Translated into more usable terms this means that the amount of water vapour usually varied between 3.3 mm and 1.6 mm. On a whole, transmission was best in July and August which is possibly due to the season, winter bringing along less humidity.

To conclude, La Silla appears to be a good site for mm-wave observations, with 230 GHz transmissions very often between 80 % and 90 % (3.3 mm to 1.6 mm H₂O). We have noted, however, that the observed atmospheric temperature profile depends on the azimuth of the observations. Practically all temperatures measured in a SW direction increase with increasing secz. As a contrast, in the east the temperature profile in many cases deviates systematically from what we expect in that it is partly inverted. This difference may be due to the fact that in the

east one is looking towards the Andes mountain range while in the SW the topology of the land is different, which may cause a difference in H₂O concentration. This interpretation is somewhat complicated by the fact that the CAT features a Nasmyth mirror, which has a slightly different vignetting at different azimuths, possibly causing the efficiency factor to differ accordingly. We are not able to estimate the influence of this effect on the basis of presently available material.

Acknowledgement

We are very much indebted to the people of the technical staff at La Silla, who were always willing to give their support when problems arose.

Reference

Lidholm, S. and de Graauw, Th: 1979, Fourth International Conference on Infrared and Millimeter Waves and their Applications, Florida 1979, p. App. 38.

A New System to Eliminate Gear Backlash in Telescopes

J. F. R. van der Ven, ESO-La Silla

Preloading a telescope geardrive, to eliminate backlash, always has been a major design aspect in telescope engineering. One of the oldest systems was to preload each axis with a steel cable, wrapped around the axis and loaded with a sufficient heavy weight, to keep the mating flanks of the gearwheel in contact under all circumstances, e.g. during windforces, unbalance, etc.

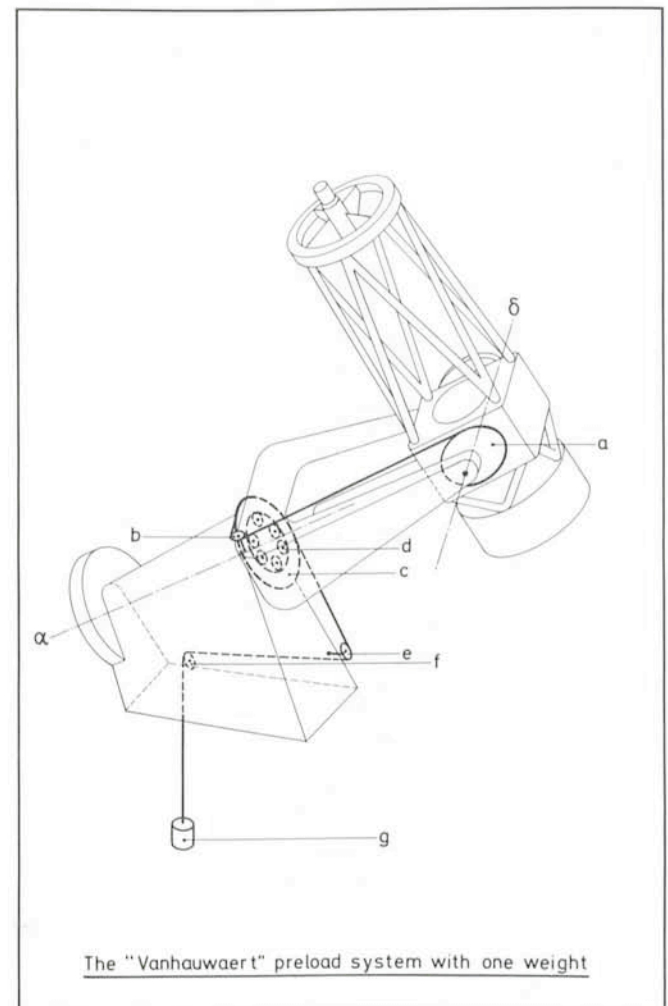
This system is still in use. To preload the polar axis is quite simple, but for the declination axis, it requires a number of rollers to guide the cable inside the polar axis. In several cases this gives problems, due to the necessary cabling, oilducts, etc., that have to pass also.

Therefore, other systems have been applied, e.g. splitgears, double-gear systems, etc. The disadvantage is the extra friction that results. Preloading the gears by two counteracting motors on each of the axes is often applied today. It is however a rather expensive solution. Besides these systems, there are more. It is not the place here to go into all of them in detail.

Mr. Vanhauwaert, of the Astro Workshop at La Silla, got an interesting idea to preload both telescope axes with one weight, that moreover avoids passing of the cable inside the polar axis. This idea is illustrated by the sketch and functions as follows:

The cable disk A is rigidly attached to the telescope tube. The cable end is fixed to this disk. The cable, loaded by weight G, is guided by cable roller B, and passes the big ring-shaped disk C. Further it is guided by the rollers E and F. The main features of this system are the roller B, that is fixed on the fork, and the ring-shaped disk C that can rotate freely about the polar axis over the rollers D. The preload moment about the polar axis results from the cable force at roller B multiplied by the distance between this force and the polar axis centre.

This system has been realized on one of the telescopes



The "Vanhauwaert" preload system with one weight

at La Silla about half a year ago, and proved to function very well.